Water Air Soil Pollut (2020) 231: 565
https://doi.org/10.1007/s11270-020-04934-y

Facile Preparation of Thiolated Reduced Graphene Oxide Aerogels for Efficient Removal of Cu(II) Ion from Water

Jie Li · Jianjun Bao

Received: 27 March 2020 / Accepted: 17 November 2020 / Published online: 26 November 2020

Abstract In our research, thiolated reduced graphene oxide aerogels (TrGOAs) was successfully prepared by using graphene oxide (GO) as precursor and sodium hydrosulfide (NaSH) as reductant via a one-pot one-step hydrothermal route under normal pressure and a subsequent freeze-drying, used as a novel carbon-based adsorptive material for adsorbing Cu(II) ions from deionized water. These aerogels show excellent adsorption ability towards Cu(II) ions, which have a huge adsorption amount around 421.21 $mg{\cdot}g^{-1}$. We studied the mechanism of the adsorption process of TrGOA-5, and the results found that the pseudo-second-order kinetic model and the Freundlich isotherm model were able to describe this process well. We also explored the interference of pH values in copper ion solutions during this adsorption process, suggesting that increasing pH is good for obtaining a higher adsorption capacity. In addition, solid-liquid separation can be readily realized by filtration and centrifugation after the end of the adsorption experiment. Overall, this research offers a relatively simple and cut-price strategy to obtain thiolated reduced graphene oxide aerogels, and these novel graphene-based adsorbents have a superior adsorption ability and recyclability in segregating copper ions from polluted water.

J. Li · J. Bao
State Key Laboratory of Polymer Materials Engineering, Polymer Research Institute, Sichuan University, Chengdu 610065, China

J. Li · J. Bao (✉)
Research Center for Application of Graphene, Sichuan University-WuXi, Wuxi 214000, China
e-mail: jjbao2000@sina.com

Keywords Graphene aerogel · Thiolated · Cu(II) · Absorption

1 Introduction

A large amount of metals are introduced into the aquatic system and cause water pollution mainly because of human activities such as overexploitation and processing of mineral resources and the massive use of chemical fertilizers and pesticides. The most common heavy metal contaminants are copper, mercury, lead, chromium, cadmium, zinc, and tin (Shen et al. 2013; Zhao et al. 2013). Among them, copper is one of the major toxic metal contaminants ions emanating from mining, chemical and mechanical polishing, metal finishing, and especially electroplating industries. Excess copper ions in surface water and groundwater are very detrimental to the biological health of nature. In the case of very low copper ion concentration, the toxicity of the aqueous solution is still relatively large, so it is necessary to reduce the concentration of copper ions in the wastewater before it can be discharged into the uncontaminated water (Dong et al. 2015; Al-Saydeh et al. 2017).

Up to now, lots of investigators have dedicated to purify the contaminated water containing heavy metal ions, and a variety of corresponding wastewater treatment methods such as adsorption (Zhao et al. 2015a), ion exchange (Alyuz and Veli 2009), flocculation (Liang et al. 2014), and chemical precipitation (Sommella et al. 2015) have been developed to purify the wastewater. As far as we know, the separation of

heavy metal pollutants from contaminated water by adsorption method has been extensively studied, which attributed to its extensive practicality, small equipment footprint, and comparable low investment costs and so forth (Liu et al. 2016). Accordingly, already multiple adsorbents such as activated carbon (Kobya 2004), zeolite (Biškup and Subotić 2005), and carbonaceous materials (Sun et al. 2013) have been prepared for treating heavy metal pollutants.

Graphene and its derivatives are a new kind of carbon-based materials that are expected to be ideal nanosorbents for removing toxic transition metal ions. These nanosorbents are of great value for the treatment of heavy metal ions because of their outstanding mechanical strength, huge surface area, and excellent chemical properties (Yanwu et al. 2011; Li and Kaner 2008; Fan et al. 2010). However, due to the intermolecular forces such as π-π stacking between these two-dimensional (2D) materials, it is easy to agglomerate and significantly impairs their adsorption performance. Graphene-based adsorbents also have secondary pollution problems during the separation process in practical applications (Chowdhury and Balasubramanian 2014). In a certain way, the 2D crystalline graphene sheets can be connected to each other and assembled in layers to obtain the 3D interconnected porous structure, which has been significantly mitigated this problem. 3D graphene-based aerogels with highly interconnected porous, tunable pore size, and low density have a broader application prospect in heavy metals removal. Importantly, the 3D graphene-based aerogels have a certain degree of hydrophobicity due to the reduction of most polar groups, thus ensuring easy separation of solid and liquid after the adsorption process. Wu et al. reported a 3D-SRGO aerogel that was prepared by adding uniformly dispersed aqueous solutions of rGO aerogel to diazonium salt solutions, which was applied to cadmium removal from wastewater. Its maximum adsorption capacity for cadmium ion calculated by Langmuir equation was up to 234.8 $mg \cdot g^{-1}$ (Wu et al. 2015).

Although 3D graphene-based aerogel adsorbents have displayed the advantages of treating wastewater containing heavy metal ions, a higher adsorption performance level is still needed to handle the increasing surge of metal ion from wastewater. Thiol and its derivatives belong to Lewis bases and thus can form stable coordination covalent bonds with Lewis acids like some key heavy metal ions. Therefore, the introduction of thiol functional groups into materials can greatly improve its adsorption capacity of transition metal ions and avoid the re-dissolution of the absorbed heavy metal ions into the purified water as much as possible, thereby rendering it a superior adsorbent for toxic metal removal (Mukherjee et al. 2016; Ding et al. 2014; Xia et al. 2017). Zhao et al. obtained S-doped graphene sponge fabricated by hydrothermal treatment of a mixed aqueous solution of graphene oxide and L-cystine; this sponge has a great adsorbability of 228 $mg \cdot g^{-1}$ capacity towards copper ion (Zhao et al. 2015b). A. Santhana Krishna Kumar et al. synthesized thiol-functionalized GO by drying a mixture of graphene oxide and mercaptobenzothiazole (MBT), the equilibrium adsorption data of the adsorbed mercury ions by this material match well with the Langmuir model, and the corresponding adsorption amount was 107.52 $mg \cdot g^{-1}$ (Krishna Kumar et al. 2016). Liu et al. fabricated thiol-functionalized magnetic graphene thanks to the (3-mercaptopropyl)trimethoxysilane (MPTES). The M-Fe_3O_4-GO composite as an adsorbent showed a huge adsorption amount for cadmium ion of 125.00 $mg \cdot g^{-1}$ (Liu et al. 2015).

However, these methods are not entirely satisfactory for the preparation of various thiol-functionalized composite, as extra regents are used and multiple preparation routes are needed. In view of the above, it is highly required to seek cheaper and more effective technique to prepare thiol-functionalized materials. Pham et al. has proposed a direct synthesis method for thiol-functionalized reduced graphene oxide by heating GO and P_4S_{10} in DMF solution (Pham et al. 2013). But P_4S_{10} is a combustible solid and easily ignited by heat, friction, or when in contact with acid, water, or moist air. Choi et al. reported that NaSH is used as a reduction and thiolating reagent to prepare a metal-decorated graphene oxide catalyst (GOSH-Ag), which was applied to decarboxylation cycloaddition reaction (Kim et al. 2012). Inspired by these works, we present a novel strategy to fabricate thiolated reduced graphene oxide aerogels (TrGOAs) by chemical reduction self-assembly using graphene oxide as precursors. The entire synthesis process is carried out in deionized water under normal pressure with the advantage of being very low cost, mild synthesis conditions, and facile preparation routes. As a reducing agent and SH-loaded modifier, NaSH can simultaneously achieve reduction and thiol-based modification of oxidizing group on the GO skeleton. The rGO sheets were then self-assembled to obtain a three-dimensional (3D) macrostructure, which was finally

freeze dried to obtain the target aerogel. Furthermore, the adsorption mechanism of TrGOA on Cu(II) ions was analyzed by isotherms and kinetic tests, and we also studied the interference of pH value of Cu(II) ions aqueous solution on adsorption capacities.

2 Experimental

2.1 Materials

GO powders were purchased from The Sixth Element Materials Technology Co., Ltd. in Changzhou, China. Sodium hydrosulfides were offered from Best-reagent Co., Ltd. in Chengdu, China. Ammonium citrate tribasic was supplied by Micxy Chemical Co., Ltd. in Chengdu, China. Ethanol, hydrochloric acid (HCl), sodium hydroxide (NaOH), ammonium hydroxide ($NH_3 \cdot H_2O$), ascorbic acid (L-aa), ammonium chloride (NH_4Cl), $Cu(NO_3)_2 \cdot 3H_2O$, and bis(cyclohexanone)oxalyldihydrazone (BCO) (analytical grade) were provided by Kelong Chemical Reagent Co., Ltd. in Chengdu, China. The distilled water applied in all tests was self-made.

2.2 Methods

2.2.1 Preparation of Thiolated Reduced Graphene Oxide Aerogels (TrGOAs)

Typically, stable GO dispersion was obtained by adding a known mass of graphite oxide powder in deionized water (6 mg/mL) and then sonicating for 1 h. Then, a fixed amount of NaSH aqueous solution was dissolved in the solution (10 mL) containing GO in a 20-mL vial and stirred for several minutes. Shortly thereafter, rGO hydrogel can be acquired by heating the above mixture at 65 °C for 7 h without stirring. The resulting hydrogel was allowed to stand for a while and naturally cooled to room temperature; it was then immersed with 200 mL of solvent composed of water and ethanol with a fixed volume ratio (4:1) for 2 days. In this period of time, the ethanol aqueous solution was changed at regular intervals. Finally, the TrGOA sample was obtained after 48 h of freeze-drying. Different initial mass ratios of GO to NaSH (1/1, 1/3, and 1/5) were used, and these thiolated reduced graphene oxide aerogels were designated as TrGOA-1, TrGOA-3, and TrGOA-5, respectively. For comparison, the graphene aerogel was prepared by the same procedures using sulfur-free ascorbic acid.

2.2.2 Adsorption Experiments

A series of adsorption experiments of TrGOA-5 on Cu(II) ions were performed in deionized water, which all following the same procedure: Firstly, put 7 mg of target adsorbent into the conical flask containing a known concentration of Cu^{2+} solution (50 mL). Thereafter, the mixture oscillated under the action of a constant temperature bath oscillator (35 °C). At a certain time, the adsorption mixture was filtered with 0.45-μm filter membrane, followed by centrifugation at 12000 rpm for 3 min. Finally, supernatant would be diluted to a certain multiple and tested for copper ions concentration by spectrophotometry with BCO (Yang et al. 2010).

The isotherm study for the adsorption process was carried out by changing concentrations of Cu^{2+} solutions, and all kinetic experiments were conducted at different adsorption time. In addition, in order to explore the interference of pH values in copper ion solutions during this adsorption process, the initial pH of each Cu^{2+} solution was changed by dropping an appropriate amount of acid or alkali aqueous solutions. The amount of Cu^{2+} adsorbed by TrGOA-5 can be obtained by the following equation:

$$q_e = \frac{(C_0 - C_e)V}{m} \quad (1)$$

where C_0 ($mg \cdot L^{-1}$) and C_e ($mg \cdot L^{-1}$) stand for the initial and equilibrium concentrations of Cu^{2+} solutions, respectively. V (mL) denotes the volume of Cu^{2+} solutions, and m (mg) represents corresponding mass of TrGOA samples.

2.2.3 Characterization

The functional groups and chemical bonds of GO and TrGOA were analyzed by XPS (XSAM800) with Al Kα as the X-ray source. The results were fitted using the XPSPeak 4.1 software. We studied the microscopic morphology of the aerogels framework via a SEM microscope (Quanta 250) at a 20 kV accelerating voltage. The chemical compositions on samples skeleton were characterized by FTIR spectroscopy (Nicolet iS50), ranging from 4000 to 400 cm^{-1}. The absorbance of all copper ion aqueous solutions was monitored by using a UV-vis

spectrophotometer (UV-2300, Hitachi), and the change in the Cu^{2+} concentrations was quantitatively analyzed.

3 Results and Discussion

3.1 Characterization of TrGOA

Detailed preparation procedure of the thiolated reduced graphene oxide aerogel (TrGOA) with a regular cylindrical geometry shown in Fig. 1 involved several typical steps. According to the digital photos of the three aerogels (Fig. 2), it is obviously that the volume of TrGOAs increases when these aerogels were functionalized with increasing amounts of NaSH. SEM was applied for further understanding the effects of GO/NaSH mass ratios (1:1, 1:2, and 1:5) on the microscopic structure of corresponding produced samples. Figure 3 shows the SEM pictures of the three samples, respectively.

As can be clearly observed that after reduction by NaSH, arbitrarily oriented, the GO flakes of the TrGOAs are assembled to interpenetrate 3D network-like structures and build lots of continuous microporous in the micrometer size range (Hou et al. 2018). Furthermore, upon increasing the content of NaSH, the pore sizes of these aerogels become slightly larger, indicating that a looser porous structure can be obtained. Comparing with other two aerogels, the TrGOA-5 sample possesses a more homogeneous pore distribution, and rich macropores embed in the aerogel imply a high specific surface area, which plays a vital role in providing more binding sites for effective adsorption (Han et al. 2014), thus chosen to further study the characterization and all adsorption experiments.

The covalent linking between GO and NaSH was confirmed by FTIR. Figure 4 a displays the FT-IR spectra of GO and TrGOA-5. For pure GO powder, it presents some typical absorption peaks; the peaks around 3368, 1731, and 1412 cm^{-1} belong to the hydroxyl, carbonyl, and carboxyl; other absorbance bands at 1618, 1224, and 1052 cm^{-1} are derived from the stretching vibrations of C=C (aromatic), C-O (epoxy), and C-O (alkoxy), respectively (Wee and Hong 2014; Tajima et al. 2017; Min et al. 2014). C–S stretching and C–SH bending of TrGOA-5 can be observed at 669 and 808 cm^{-1} (Pham et al. 2013), which suggests that thiol functional group of NaSH have been covalently grafted on the rGO surface. The intensity of some peaks in the aerogel spectrum is significantly lower, including peaks at 3431 cm^{-1}, 1698 cm^{-1}, and 1384 cm^{-1} (Hu et al. 2013a). These results indicate that the chemical reactions may occur between the –SH groups in NaSH and –OH groups on GO surface. Furthermore, the signals in

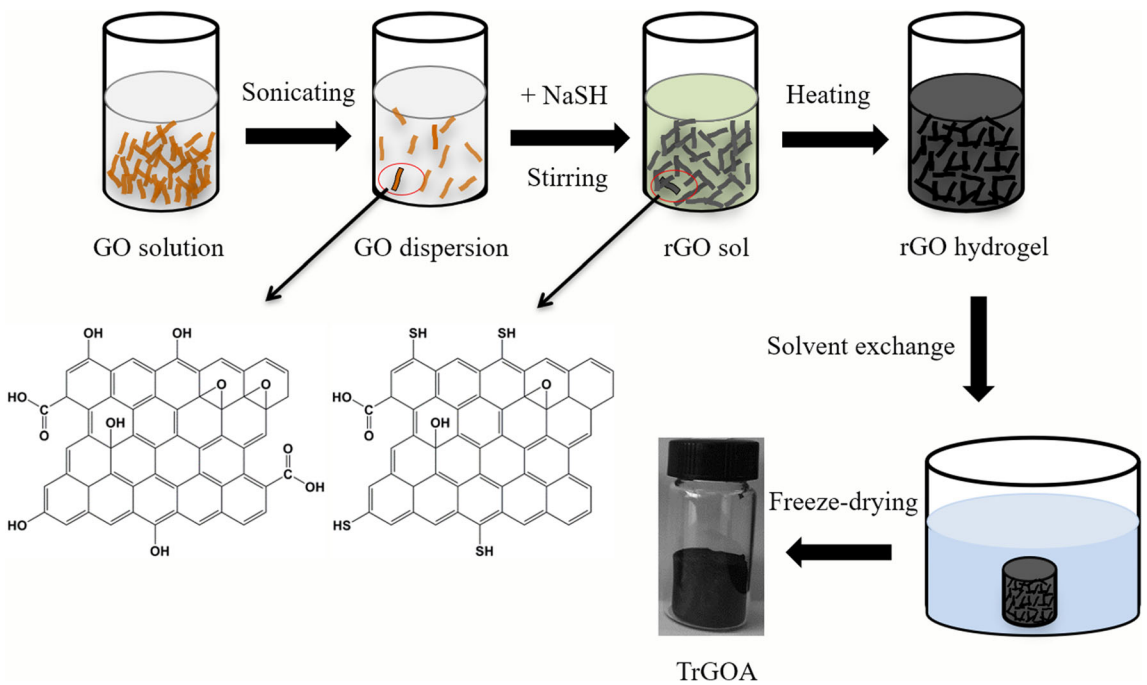

Fig. 1 Schematic illustration of thiolated reduced graphene oxide aerogels (TrGOA)

the spectrum between 1100 and 1300 cm^{-1} correspond to the C–O–C stretching (Wee and Hong 2014), demonstrating that there are still plenty of oxidizing groups on this modified aerogel; that is, the GO nanosheets have been partially reduced by NaSH during the functionalization treatment.

XPS analysis was performed to investigate significant chemical bonding and sulfur content of TrGOA-5. The high-resolution C1s peaks of TrGOA-5 in Fig. 4b contains four peaks of 284.6, 285.5, 286.6, and 288.3 eV, which represent the C=C, C–C, C–O/C–S, and C=O bonds, respectively (Zhang et al. 2017; Tian et al. 2015). Compared to the C1s XPS spectrum of GO, the intensity of binding energies of some oxidizing groups significantly decreased in the C 1 s spectrum of TrGOA-5 (Fig. 4c). The phenomenon is consistent with that the C/O atomic ratios (5.7) of TrGOA-5 is higher than that of GO (2.5), and this result can serve as a message that most oxygenated groups have been reduced by NaSH during the chemical processing.

We further analyzed the high-resolution S 2p peaks of TrGOA-5. Two main characteristic peaks with 1.2 eV splitting appear in Fig. 4d. The peaks with a high binding energy of 163.8 eV and the lower one at 165.0 eV are attributed to H–C–S and R–C–S in the aerogel, respectively (Chen et al. 2016; Lashkor et al. 2014). The broad peak occurs at 168.8 eV is ascribed to S–O_3, which is caused by the oxidation of –SH groups in air (Neal et al. 2001). It is worth mentioning that the sample tested by XPS has a sulfur content of 5.13 at %, of which the thiol group accounts for 2.44%. This result has a major impact on increasing the equilibrium adsorption amount of Cu^{2+}.

The above information further corroborates that C–S covalent bonds and –SH groups are successfully introduced onto the backbone of TrGOA by using a simple chemical method. We speculate that the TrGOA with so many adsorption sites should show great potential to effectively adsorb heavy metal ions as an adsorptive material.

3.2 Adsorption Studies

3.2.1 Adsorption of Cu^{2+} on TrGOA

In order to test the contribution of thiol groups in adsorption experiments, we designed a comparative experiment. TrGOA-5 and graphene aerogel without thiol

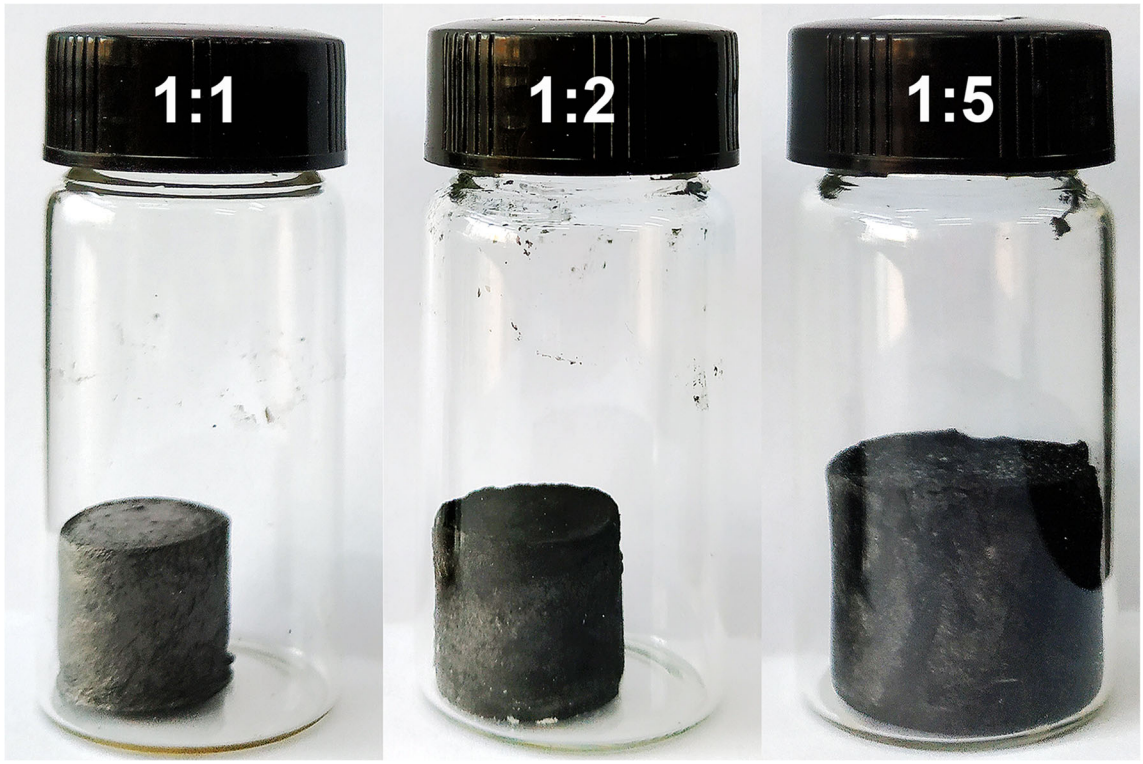

Fig. 2 Three digital photos of the TrGOAs with different GO/NaSH mass ratio

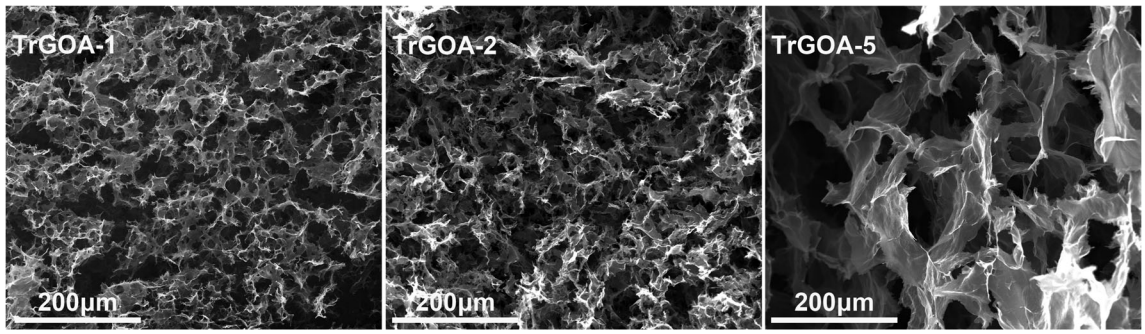

Fig. 3 Three SEM micrographs of TrGOA samples

group (–SH) were shaken in Cu(II) ion solutions for 12 h (temperature: 35 °C, pH: 5.5, concentration: 550 mg·L^{-1}); the equilibrium adsorption amounts of the two aerogels were 421.21 and 79.00 mg·g^{-1}, respectively. This result obviously indicates that thiol groups have a profound effect on improving adsorption performance of rGO aerogels. The huge adsorption capacity of TrGOA-5 samples for Cu(II) ions can be explained as follows: (1) the residual oxidizing groups and abundant thiol groups on the TrGOA-5 framework have the opportunity to act as binding sites for interaction with Cu(II) ions, thereby enhancing the ability of TrGOA-5 to remove Cu(II) ions. (2) Physical adsorption may also be one of the adsorption mechanisms; three-dimensional porous structure of the TrGOA-5 provides sufficient ion transportation channels, promoting the migration and penetration of Cu(II) ions into interior of the adsorptive material. Moreover, the huge specific surface area is inclined to offer remarkable active adsorption sites (Han et al. 2018). In summary, the unique chemical

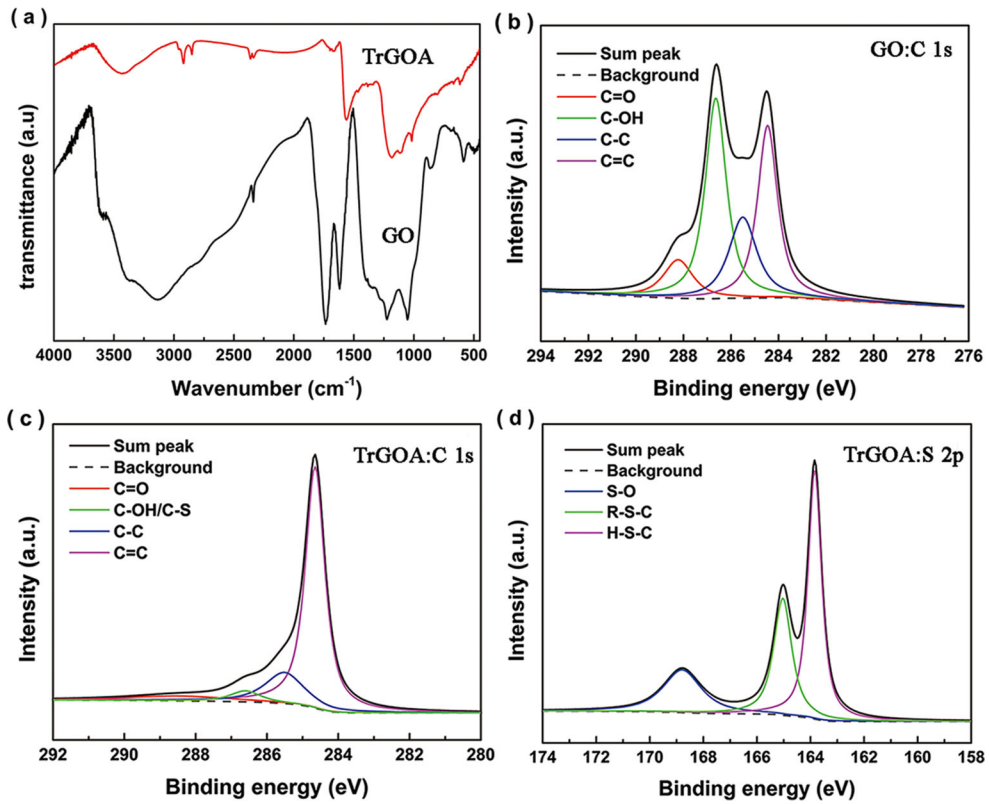

Fig. 4 Characterization of GO and TrGOA: (**a**) FT-IR spectra, (**b**) (**c**) XPS C1s, and (**d**) S 2p core-level spectra of TrGOA-5

and physical properties make TrGOA-5 have a better adsorption performance for Cu(II) ions.

3.2.2 Adsorption Kinetics

Adsorption kinetics contributes to a detailed study of adsorption process and mechanism of this adsorbent. For this purpose, bath kinetic experiments were measured by varying the contact time during the adsorption process. These experiments were conducted herein at pH 5.5 and initial Cu^{2+} concentration 250 mg·L^{-1}. Figure 5 a displays the adsorption behaviors of TrGOA-5 for copper ions; the curve consists of a fast initial phase and a slower adsorption rate. This phenomenon is mainly caused by the fact that the TrGOA-5 sample contained enough effective adsorption sites at the beginning of this adsorption process; thus, numerous copper ions tend to be adsorbed quickly by this adsorbent. As the adsorption time is prolonged, the adsorption rate becomes slower owing to the decrease of available adsorbent active sites and eventually reaches equilibrium (Pan et al. 2018).

The pseudo-second-order can be employed to fit adsorption data obtained after the kinetic experiments are completed. The linear equation of this model can be presented as follows (Wang et al. 2019):

$$\frac{t}{q_t} = \frac{1}{k_2 q_e^2} + \frac{t}{q_e} \tag{2}$$

where adsorption amount of TrGOA-5 at t and equilibrium are represented by q_t (mg·g^{-1}) and q_e (mg·g^{-1}), respectively. Pseudo-second-order kinetic rate constant is represented by k_2 (g·mg^{-1}·min^{-1}).

Figure 5 b displays the fitting curve based on the pseudo-second-order model. It is easy to get q_e and k_2 values from that curve. The pseudo-first-order rate reaction model is also used to test experimental data. The rate constant k_1 is determined by fitting the same data of copper adsorption to pseudo-first-order kinetic expression (Nguyen et al. 2009). k_1 and k_2 are listed in Table 1. The experimental data of the Cu(II) ions adsorption by TrGOA-5 can be perfectly matched to the pseudo-second-order due to its high correlation coefficient (R^2). Moreover, there is a quite low relative error between the calculated adsorption capacity (317.46 mg·g^{-1}) from pseudo-second-order formula and its actual adsorption data of q_e (306.00 mg·g^{-1}).

The above conclusions fully demonstrate that the pseudo-second-order has an ability to systematically describe the adsorption kinetic behavior of Cu(II) ions by TrGOA-5, supporting the hypothesis that the main rate step of adsorption process may be ruled by chemical adsorption, which is similar to most previous reports on other thiol modified adsorptive material (Geng et al. 2017).

3.2.3 Adsorption Isotherm

Adsorption isotherm studies prefer to understand the interaction between divalent copper ions and TrGOA-5 during the adsorption process. Corresponding experiments were performed by using various Cu(II) ions concentration while the temperature, pH, and adsorption time were kept at 35 °C, 5.5, and 12 h. The results presented in Fig. 6a show that with increase at the initial concentration of Cu^{2+} in deionized water, adsorption capacities of the aerogel sample increase from 92.86 to 421.21 mg·g^{-1} accordingly. The high concentration of Cu^{2+} aqueous solution increases the chance of effective

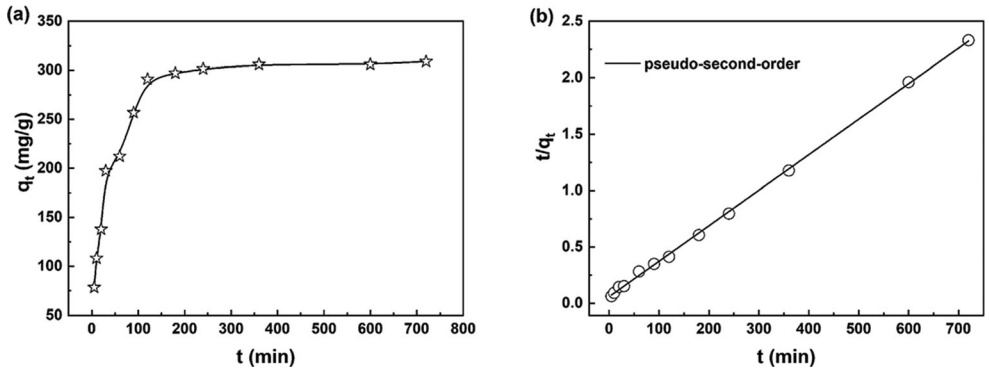

Fig. 5 (**a**) Adsorption kinetics curves of Cu^{2+} on uptake of TrGOAs-5 (35 °C) and (**b**) pseudo-second-order fitted curve

Table 1 Rate constants for first- and second-order rates of copper adsorption on TrGOAs

Adsorbate	Q_{exp} (mg/g)	Pseudo-first-order model			Pseudo-second-order model		
		q_{1e} (mg/g)	k_1 (min^{-1})	R_1^2	q_{2e} (mg/g)	k_2 ($g \cdot mg^{-1} \cdot min^{-1}$)	R_2^2
Cu^{2+}	306.00	184.70	0.01	0.9535	317.46	1.17×10^{-4}	0.9994

contact between Cu^{2+} and some functional groups of TrGOA-5 and also facilitates the entry of Cu^{2+} into the adsorbent interior. Importantly, a maximum adsorption capacity reaches when the Cu^{2+} concentration is about 550.0 $mg{\cdot}L^{-1}$.

Three adsorption models, include Langmuir, Freundlich, and Temkin, are used to describe the adsorption process. Langmuir model considers that the adsorption process occurs on a homogeneous surface by single layer adsorption (Alyuz and Veli 2009). The model can be written in the following expression:

$$\frac{C_e}{q_e} = \frac{C_e}{q_{max}} + \frac{1}{k_L q_{max}} \tag{3}$$

where q_e and q_{max} represent adsorption amount at the equilibrium and maximum adsorption amount ($mg{\cdot}g^{-1}$), respectively. C_e stands for equilibrium concentration of Cu^{2+} ($mg{\cdot}L^{-1}$), and k_L represents the rate constant of pseudo-second-order equation.

Freundlich model is commonly applied to show multilayer adsorption on a heterogeneous surface (Huang and Yan 2018). The equations can be expressed in the following expression:

$$\ln q_e = \ln k_F + \frac{1}{n} \ln C_e \tag{4}$$

where k_F and $1/n$ belong to Freundlich model constant and influence coefficient, which are associated with adsorption amount and intensity, respectively. When

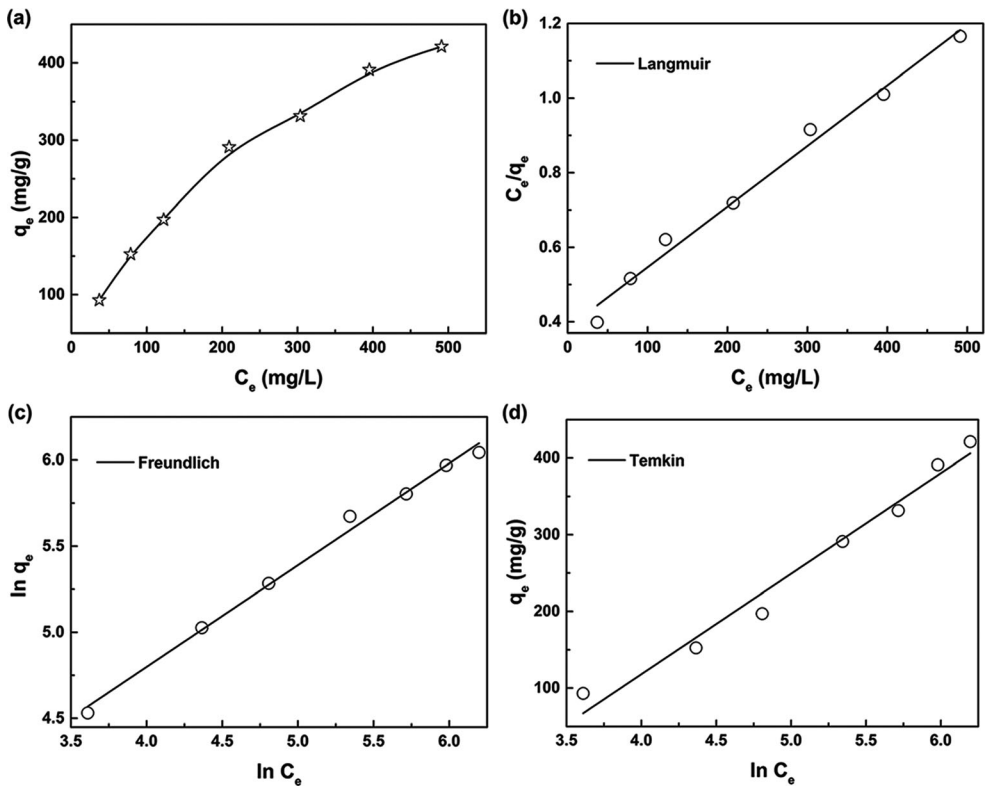

Fig. 6 Adsorption of TrGOAs-5 towards Cu(II) ions. (**a**) Adsorption isotherm, (**b**) Langmuir isotherm, (**c**) Freundlich isotherm, and (**d**) Temkin isotherm

Table 2 Adsorption amount of different adsorbent materials for copper ions

Adsorbent materials	Amount ($mg \cdot g^{-1}$)	Ref.
Ion-exchange resin	73.77	(Nguyen et al. 2009)
GO	46.60	(Yang et al. 2010)
GO aerogel	19.65	(Mi et al. 2012)
GO/PAA hybrid aerogels	390.34	(Han et al. 2018)
CGGO aerogel	130.00	(Zhang et al. 2011)
S-doped GS	228.00	(Zhao et al. 2015b)
SMGO composite	62.73	(Hu et al. 2013b)
GO-SH	99.17	(Chen et al. 2016)
CS/GO-SH composite	425.00	(Li et al. 2015)
TrGOA	421.21	This work

numerical values of $1/n$ are between zero and one, there will be a favorable adsorption system (Alyuz and Veli 2009).

Temkin isotherm believes that the adsorbing species-adsorbent interactions have a greater impact on the adsorption process (Huang et al. 2018), which can be written as:

$$q_e = B \ln k_T + B \ln C_e \quad (5)$$

where B represents Temkin constant, which is associated with the heat of adsorption, and k_T represents equilibrium binding constant.

The linear curves based on the above three equations in Fig. 6b–d can be obtained by fitting experimental data. Some isotherm constants and correlation coefficients (R^2) of those equations displayed in Table 1 can be calculated from corresponding fitting curves and results. From all fitting results, the R^2 values of the Langmuir, Freundlich, and Temkin models have a very high value, indicating that all of them can simulate the isothermal adsorption process quite well. The R^2 value of Freundlich is the highest compared to the other two models; that is, the Freundlich model appears to match isothermal adsorption data best. Moreover, the calculated $1/n$ value of Freundlich is significantly less than 1. The above conclusions suggest that the adsorption process of Cu^{2+} by TrGOA-5 is carried out on its heterogeneous surface.

Furthermore, we compared maximum adsorption capacity of TrGOA for Cu(II) ions with other adsorbent materials reported before, which is presented in Table 2. As stated in the table, the adsorption amount of TrGOA-5 for Cu(II) ions in our work is significantly higher than that of most other materials, suggesting that the adsorbent based on thiolated reduced graphene oxide aerogel has potential application value for adsorbing metal copper ion in water.

3.3 Interference of pH Value

The pH value in solutions affects surface charges and protonation of some chemical groups of TrGOA, as well as the ionic state of metal copper; it is thus a significant factor in the adsorption process. The interference of pH on the removal of Cu^{2+} was studied at a pH of 1.5–5.5 and a concentration of 250 $mg \cdot L^{-1}$.

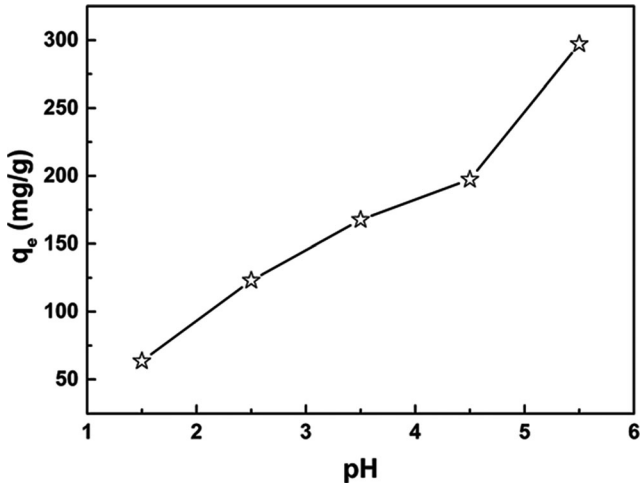

Fig. 7 The interference of pH on the removal of Cu^{2+} by TrGOA-5

Similar to the above description, Fig. 7 exhibits a gradual increase in adsorption ability for Cu^{2+} with the increase in pH values. This illustrates that solution pH value is directly related to the adsorption performance of TrGOA for Cu^{2+}. When the pH is very low, because of the presence of empty orbitals in both H^+ and Cu^{2+}, excess H^+ has an advantage over Cu^{2+} when competing for binding sites on the TrGOA surface (Mi et al. 2012). In addition, most surface groups of the adsorbent would be protonated which induces an electrostatic repulsion of Cu^{2+}, resulting in a low adsorption amount towards metal ion.

Subsequently, the concentration of H^+ gradually decreases, which is propitious to the metal ion adsorption. Additionally, the surface of TrGOA acquired more negative charges, which can enhance the electrostatic attraction with the positive charge of Cu^{2+} to promote the adsorption process (Han et al. 2018). That is to say, there would be more effective active sites on the aerogel framework combined with more divalent metal copper ion; therefore, the adsorption amount of copper ions has increased significantly.

4 Conclusions

In our research, a new thiolated reduced graphene oxide aerogel (TrGOA) was successfully fabricated through a facile chemical reduction self-assembly process under atmospheric pressure and a low temperature. TrGOA-5 was designated as an adsorbent sample to study the adsorptive property of copper ions in water. The adsorbent displayed a greatly improved performance for adsorption compared to most previously reported conventional materials, which depends on its highly interconnected porous, huge internal surface area and multiple exposed active adsorption sites. Kinetic study showed that the adsorption process of TrGOA-5 for Cu(II) ions fits well with the pseudo-second-order equations, indicating that the adsorption process tends to be chemisorbed, and the results of adsorption isotherm study fits well with the Freundlich isotherm equations, suggesting that Cu(II) ions formed a multilayer adsorption on TrGOA-5 surface. A high solution pH value was beneficial for the removal of Cu(II) ions in water by TrGOA-5. Based on all above findings, the thiolated reduced graphene oxide aerogel prepared by this simple synthesis strategy could potentially be an ideal candidate adsorbent for efficiently adsorbing Cu(II) ions from contaminated water.

Acknowledgments The authors highly appreciate the State Key Laboratory of Polymer Materials Engineering for all the tests and the Analytical & Testing Center of Sichuan University for XPS work.

Compliance with Ethical Standards

Conflict of Interest The authors declare that they have no conflicts of interest.

References

Al-Saydeh, S. A., El-Naas, M. H., & Zaidi, S. J. (2017). Copper removal from industrial wastewater: A comprehensive review. *Journal of Industrial and Engineering Chemistry, 56*, 35–44.

Alyuz, B., & Veli, S. (2009). Kinetics and equilibrium studies for the removal of nickel and zinc from aqueous solutions by ion exchange resins. *Journal of Hazardous Materials, 167*, 482–488.

Biškup, B., & Subotić, B. (2005). Removal of heavy metal ions from solutions using zeolites. III. Influence of sodium ion concentration in the liquid phase on the kinetics of exchange processes between cadmium ions from solution and sodium ions from zeolite a. *Separation Science and Technology, 39*, 925–940.

Chen, D., Zhang, H., Yang, K., & Wang, H. (2016). Functionalization of 4-aminothiophenol and 3-aminopropyltriethoxysilane with graphene oxide for potential dye and copper removal. *Journal of Hazardous Materials, 310*, 179–187.

Chowdhury, S., & Balasubramanian, R. (2014). Recent advances in the use of graphene-family nanoadsorbents for removal of toxic pollutants from wastewater. *Advances in Colloid and Interface Science, 204*, 35–56.

Ding, Z., Hu, X., Morales, V. L., & Gao, B. (2014). Filtration and transport of heavy metals in graphene oxide enabled sand columns. *Chemical Engineering Journal, 257*, 248–252.

Dong, Z., Zhang, F., Wang, D., Liu, X., & Jin, J. (2015). Polydopamine-mediated surface-functionalization of graphene oxide for heavy metal ions removal. *Journal of Solid State Chemistry, 224*, 88–93.

Fan, Z., Yan, J., Zhi, L., Zhang, Q., Wei, T., Feng, J., Zhang, M., Qian, W., & Wei, F. (2010). A three-dimensional carbon nanotube/graphene sandwich and its application as electrode in supercapacitors. *Advanced Materials, 22*, 3723–3728.

Geng, B., Wang, H., Wu, S., Ru, J., Tong, C., Chen, Y., Liu, H., Wu, S., & Liu, X. (2017). Surface-tailored nanocellulose aerogels with thiol-functional moieties for highly efficient and selective removal of Hg(II) ions from water. *ACS Sustainable Chemistry & Engineering, 5*, 11715–11726.

Han, Z., Tang, Z., Shen, S., Zhao, B., Zheng, G., & Yang, J. (2014). Strengthening of graphene aerogels with tunable density and high adsorption capacity towards Pb2+. *Scientific Report, 4*, 5025.

Han, Q., Chen, L., Li, W., Zhou, Z., Fang, Z., Xu, Z., & Qian, X. (2018). Self-assembled three-dimensional double network graphene oxide/polyacrylic acid hybrid aerogel for removal of cu(2+) from aqueous solution. *Environmental Science and Pollution Research, 25*, 34438–34447.

Hou, P., Xing, G., Han, D., Wang, H., Yu, C., & Li, Y. (2018). Preparation of zeolite imidazolate framework/graphene hybrid aerogels and their application as highly efficient adsorbent. *Journal of Solid State Chemistry, 265*, 184–192.

Hu, C., Liu, Y., Yang, Y., Cui, J., Huang, Z., Wang, Y., Yang, L., Wang, H., Xiao, Y., & Rong, J. (2013a). One-step preparation of nitrogen-doped graphenequantum dots from oxidized debris of graphene oxide. *Journal of Materials Chemistry B, 1*, 39–42.

Hu, X.-j., Liu, Y.-g., Wang, H., Chen, A.-w., Zeng, G.-m., Liu, S.-m., Guo, Y.-m., Hu, X., Li, T.-t., Wang, Y.-q., Zhou, L., & Liu, S.-h. (2013b). Removal of Cu(II) ions from aqueous solution using sulfonated magnetic graphene oxide composite. *Separation and Purification Technology, 108*, 189–195.

Huang, J., & Yan, Z. (2018). Adsorption mechanism of oil by resilient Graphene aerogels from oil-water emulsion. *Langmuir., 34*, 1890–1898.

Huang, Y., Zhu, J., Liu, H., Wang, Z., & Zhang, X. (2018). Preparation of porous graphene/carbon nanotube composite and adsorption mechanism of methylene blue, SN. *Applied Sciences, 1*.

Kim, J. D., Palani, T., Kumar, M. R., Lee, S., & Choi, H. C. (2012). Preparation of reusable Ag-decorated graphene oxide catalysts for decarboxylative cycloaddition. *Journal of Materials Chemistry, 22*, 20665.

Kobya, M. (2004). Removal of Cr(VI) from aqueous solutions by adsorption onto hazelnut shell activated carbon: Kinetic and equilibrium studies. *Bioresource Technology, 91*, 317–321.

Krishna Kumar, A. S., Jiang, S.-J., & Tseng, W.-L. (2016). Facile synthesis and characterization of thiol-functionalized graphene oxide as effective adsorbent for Hg(II). *Journal of Environmental Chemical Engineering, 4*, 2052–2065.

Lashkor, M., Rawson, F. J., Preece, J. A., & Mendes, P. M. (2014). Switching specific biomolecular interactions on surfaces under complex biological conditions. *Analyst., 139*, 5400–5408.

Li, D., & Kaner, R. B. (2008). Materials science. Graphene-based materials. *Science, 320*, 1170–1171.

Li, X., Zhou, H., Wu, W., Wei, S., Xu, Y., & Kuang, Y. (2015). Studies of heavy metal ion adsorption on chitosan/sulfydryl-functionalized graphene oxide composites. *Journal of Colloid and Interface Science, 448*, 389–397.

Liang, C.-Z., Sun, S.-P., Li, F.-Y., Ong, Y.-K., & Chung, T.-S. (2014). Treatment of highly concentrated wastewater containing multiple synthetic dyes by a combined process of coagulation/flocculation and nanofiltration. *Journal of Membrane Science, 469*, 306–315.

Liu, J., Du, H., Yuan, S., He, W., & Liu, Z. (2015). Synthesis of thiol-functionalized magnetic graphene as adsorbent for cd(II) removal from aqueous systems. *Journal of Environmental Chemical Engineering, 3*, 617–621.

Liu, J., Xiao, G., Ye, X., Wang, G., Zhang, H., Zhou, H., Zhang, Y., & Zhao, H. (2016). 3D graphene/□-MnO2 aerogels for high efficient and reversible removal of heavy metal ions. *Journal of Materials Chemistry A, 4*, 1970–1979.

Mi, X., Huang, G., Xie, W., Wang, W., Liu, Y., & Gao, J. (2012). Preparation of graphene oxide aerogel and its adsorption for Cu2+ ions. *Carbon, 50*, 4856–4864.

Min, Y., Qi, X. F., Xu, Q., & Chen, Y. (2014). Enhanced reactive oxygen species on a phosphate modified C3N4/graphene photocatalyst for pollutant degradation. *CrystEngComm, 16*, 1287.

Mukherjee, R., Bhunia, P., & De, S. (2016). Impact of graphene oxide on removal of heavy metals using mixed matrix membrane. *Chemical Engineering Journal, 292*, 284–297.

Neal, A. L., Techkarnjanaruk, S., Dohnalkova, A., Mccready, D., Peyton, B. M., & Geesey, G. G. (2001). Iron sulfides and sulfur species produced at hematite surfaces in the presence of sulfate-reducing bacteria. *Geochimica et Cosmochimica Acta, 65*, 223–235.

Nguyen, N., Lee, J.-c., Jha, M., Yoo, K., & Jeong, J. (2009). Copper recovery from low concentration waste solution using Dowex G-26 resin. *Hydrometallurgy, 97*, 237–242.

Pan, L., Wang, Z., Yang, Q., Huang, R. (2018). Efficient removal of lead, copper and cadmium ions from water by a porous calcium alginate/graphene oxide composite aerogel, nanomaterials-basel 8.

Pham, C. V., Eck, M., & Krueger, M. (2013). Thiol functionalized reduced graphene oxide as a base material for novel graphene-nanoparticle hybrid composites. *Chemical Engineering Journal, 231*, 146–154.

Shen, H., Chen, J., Dai, H., Wang, L., Hu, M., & Xia, Q. (2013). New insights into the sorption and detoxification of chromium (VI) by tetraethylenepentamine functionalized nanosized magnetic polymer adsorbents: Mechanism and pH effect. *Industrial and Engineering Chemistry Research, 52*, 12723–12732.

Sommella, A., Caporale, A. G., Denecke, M. A., Mangold, S., Pigna, M., Santoro, A., Terzano, R., & Violante, A. (2015). Nature and reactivity of layered double hydroxides formed by coprecipitating Mg, Al and As(V): Effect of arsenic concentration, pH, and aging. *Journal of Hazardous Materials, 300*, 504–512.

Sun, Y., Shao, D., Chen, C., Yang, S., & Wang, X. (2013). Highly efficient enrichment of radionuclides on graphene oxide-supported polyaniline. *Environmental Science & Technology, 47*, 9904–9910.

Tajima, K., Isaka, T., Yamashina, T., Ohta, Y., Matsuo, Y., & Takai, K. (2017). Functional group dependence of spin magnetism in graphene oxide. *Polyhedron, 136*, 155–158.

Tian, W., Gao, Q., Tan, Y., Zhang, Y., Xu, J., Li, Z., Yang, K., Zhu, L., & Liu, Z. (2015). Three-dimensional functionalized graphenes with systematical control over the interconnected pores and surface functional groups for high energy performance supercapacitors. *Carbon, 85*, 351–362.

Wang, S., Ning, H., Hu, N., Huang, K., Weng, S., Wu, X., Wu, L., & Liu, J. (2019). Alamusi, preparation and characterization of graphene oxide/silk fibroin hybrid aerogel for dye and heavy metal adsorption. *Composites Part B: Engineering, 163*, 716–722.

Wee, B. H., & Hong, J. D. (2014). Multilayered poly(p-phenylenevinylene)/reduced graphene oxide film: An efficient organic current collector in an all-plastic supercapacitor. *Langmuir., 30*, 5267–5275.

Wu, S., Zhang, K., Wang, X., Jia, Y., Sun, B., Luo, T., Meng, F., Jin, Z., Lin, D., Shen, W., Kong, L., & Liu, J. (2015).

Enhanced adsorption of cadmium ions by 3D sulfonated reduced graphene oxide. *Chemical Engineering Journal, 262*, 1292–1302.

Xia, Z., Baird, L., Zimmerman, N., & Yeager, M. (2017). Heavy metal ion removal by thiol functionalized aluminum oxide hydroxide nanowhiskers. *Applied Surface Science, 416*, 565–573.

Yang, S. T., Chang, Y., Wang, H., Liu, G., Chen, S., Wang, Y., Liu, Y., & Cao, A. (2010). Folding/aggregation of graphene oxide and its application in Cu2+ removal. *Journal of Colloid and Interface Science, 351*, 122–127.

Yanwu, Z., Shanthi, M., Stoller, M. D., Ganesh, K. J., Weiwei, C., Ferreira, P. J., Adam, P., Wallace, R. M., Cychosz, K. A., & Matthias, T. (2011). Carbon-based supercapacitors produced by activation of graphene. *Science, 332*, 1537.

Zhang, N., Qiu, H., Si, Y., Wang, W., & Gao, J. (2011). Fabrication of highly porous biodegradable monoliths strengthened by graphene oxide and their adsorption of metal ions. *Carbon, 49*, 827–837.

Zhang, L., Li, H., Lai, X., Su, X., Liang, T., & Zeng, X. (2017). Thiolated graphene-based superhydrophobic sponges for oil-water separation. *Chemical Engineering Journal, 316*, 736–743.

Zhao, Y., Zhao, D., Chen, C., & Wang, X. (2013). Enhanced photo-reduction and removal of Cr (VI) on reduced graphene oxide decorated with TiO2 nanoparticles. *Journal of Colloid and Interface Science, 405*, 211–217.

Zhao, W., Tang, Y., Jia, X., & Jie, K. (2015a). Functionalized graphene sheets with poly(ionic liquid)s and high adsorption capacity of anionic dyes. *Applied Surface Science, 326*, 276–284.

Zhao, L., Yu, B., Xue, F., Xie, J., Zhang, X., Wu, R., Wang, R., Hu, Z., Yang, S. T., & Luo, J. (2015b). Facile hydrothermal preparation of recyclable S-doped graphene sponge for Cu2+ adsorption. *Journal of Hazardous Materials, 286*, 449–456.